HHS Public Access

Author manuscript

Biomacromolecules. Author manuscript; available in PMC 2018 April 10.

Published in final edited form as:

Biomacromolecules. 2017 April 10; 18(4): 1393–1400. doi:10.1021/acs.biomac.7b00118.

Patterning 3D hydrogel microenvironments using hyperbranched polyglycerols for independent control of mesh size and stiffness

Sara Pedron[1], **Amanda M. Pritchard**[1], **Gretchen A. Vincil**[2], **Brenda Andrade**[2], **Steven C. Zimmerman**[2], and **Brendan A.C. Harley**[1,3,*]

[1]Carl R. Woese Institute for Genomic Biology, University of Illinois at Urbana-Champaign, 1206 West Gregory Drive, Urbana, IL 61801, USA

[2]Department of Chemistry, University of Illinois at Urbana-Champaign, 505 South Mathews Avenue, Urbana, IL 61801, USA

[3]Dept. of Chemical and Biomolecular Engineering, University of Illinois at Urbana-Champaign, 110 Roger Adams Lab., 600 S. Mathews Avenue, Urbana, IL 61801, USA

Abstract

The extracellular matrix (ECM) is an environment rich with structural, mechanical, and molecular signals that can impact cell biology. Traditional approaches in hydrogel biomaterial design often rely on modifying the concentration of cross-linking groups to adjust mechanical properties. However, this strategy provides limited capacity to control additional important parameters in 3D cell culture such as microstructure and molecular diffusivity. Here we describe the use of multifunctional hyperbranched polyglycerols (HPGs) to manipulate the mechanical properties of polyethylene glycol (PEG) hydrogels while not altering biomolecule diffusion. This strategy also provides the ability to separately regulate spatial and temporal distribution of biomolecules tethered within the hydrogel. The functionalized HPGs used here can also react through a copper-free click chemistry, allowing for the encapsulation of cells and covalently tethered biomolecules within the hydrogel. Because of the hyperbranched architecture and unique properties of HPGs, their addition into PEG hydrogels affords opportunities to locally alter hydrogel crosslinking density with minimal effects on global network architecture. Additionally, photocoupling chemistry allows micropatterning of bioactive cues within the three-dimensional gel structure. This approach therefore enables us to tailor mechanical and diffusive properties independently while further allowing for local modulation of biomolecular cues to create increasingly complex cell culture microenvironments.

[*]**Corresponding author:** Prof. B. A. C. Harley, Dept. of Chemical and Biomolecular Engineering, Carl R. Woese Institute for Genomic Biology, University of Illinois at Urbana-Champaign, 110 Roger Adams Lab., 600 S. Mathews Avenue, Urbana, IL 61801, USA, bharley@illinois.edu.

Supporting information.

This material is available free of charge via the Internet at http://pubs.acs.org.

^{1}H NMR spectra and SEC analyses of monomers, FRAP raw data, additional 3D hydrogel patterning images, and physical properties data.

Author contributions

The manuscript was written through contributions of all authors. All authors have given approval to the final version of the manuscript.

Notes

The authors declare no competing financial interest.

TOC image

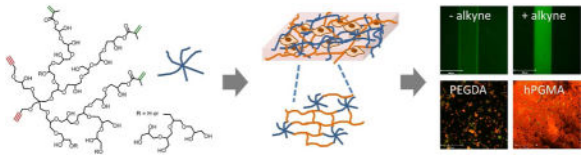

Keywords

hyperbranched polyglycerol; hydrogels; patterning; PEG; cell microenvironment; diffusion

INTRODUCTION

Tissue engineering efforts have recently targeted the development of biomaterials that provide the ability to present increasingly complex extrinsic signals to cells encapsulated within the network. A primary area of effort has been towards creating hydrogels that systematically and even spatially or temporally alter biochemical and biomechanical properties through control over macromer concentrations, polymerization conditions, and degradation kinetics.[1–4] However, the correlation between hydrogel modulus and mesh size makes it difficult to assign specific cell responses to a particular scaffold property. Traditionally, these physical properties are associated with the cross-linking density of a polymer network modulated by altering the molecular weight or concentration of PEG diacrylate (PEGDA).[5] Lower molecular weights of PEGDA monomers result in hydrogels with decreased chain length between cross-links, which translates to an increased cross-linking density, and consequently stiffer polymer network.[6] Higher concentrations of PEGDA also lead to increased cross-linking densities and therefore significant increases in modulus.[7] However, increases in modulus that result from increased cross-linking density are typically coupled with decreases in mesh size that also affect diffusivity and swelling of the network.[8] Recently, new strategies are being explored to break this relationship, such as through the addition of low concentrations of 4-arm PEG cross-linker to create local increases in cross-linking density that substantially increase the modulus while minimally perturbing bulk mesh size.[9]

Hyperbranched polyglycerols (HPGs) have a dendrimer-like architecture with a polyether scaffold and a high concentration of hydroxyl end-groups that together afford high biocompatibility.[10] These characteristics and the ability to functionalize the hydroxyl groups are very attractive in the design of new biomaterial architectures, for applications as drug carriers, molecular labels, or for the development of instructive material platforms for cell culture.[11] HPG can be regarded as analogous to the well-known polyethylene glycol (PEG), accepted in multiple biomedical applications due to its biocompatibility and its suitability as a polymer for the design of hydrogels.[12] Hydrogels made from hyperbranched polymers have been used for biomedical applications that require spatial control of cell adhesion and biomolecule encapsulation and delivery.[13, 14] Further, alkyne-cored HPGs have been used for the functionalization and stabilization of nanoparticles, as well as stabilizing agents for water-soluble fluorescent dyes.[15] Recent reports have documented the use of UV

photopolymerizable hyperbranched polyglycerols to create hydrogels with tunable mechanical properties and well defined sizes and shapes.[16, 17] Moreover, hydrogels have also been reported that combine HPG and PEG macromonomers in aqueous droplets, allowing for encapsulation of living yeast cells into the resultant microgels.[18] As a result, we hypothesize that the high functionality and compact structure of HPGs allows additional control over PEGDA hydrogel mechanical properties, without impacting hydrogel pore structure and diffusion properties.

In addition to decoupling hydrogel mechanical properties and mesh structure, multi-functional crosslinking reactions provide the opportunity to incorporate biomolecules, degradable linkers, and other functional groups to further control cell response. Khetan et al. described a technique that incorporates multiple modes of crosslinking, applied sequentially, to create spatially-resolved regions of stiffening and softening within a hydrogel network.[19] Additionally, click chemistry provides extremely selective and orthogonal reactions that can proceed with high efficiency and under a variety of mild (*e.g.*, copper-free chemistry) conditions.[20] Thiol-click reactions are a rapid, robust, and efficient immobilization strategy for creating spatially-patterned changes in the hydrogel microenvironments in real time. Further, thiol–ene and thiol–yne reactions belong to a class of click reactions that involve the free-radical-mediated addition of thiols to unsaturated carbon–carbon bonds. Although both alkene and alkyne groups can react with a single thiol group, radical additions to alkynes produce vinyl sulfides, which can undergo a second addition of a thiyl radical.[21] Thiol–ene/yne reactions are particularly useful for biological applications because thiol groups are present in cysteines, and this amino acid can easily be introduced into synthetic peptides, as well as being found in many native proteins. Thiol-yne reactions have been employed as a tool for surface modification and functionalization.[22] Brush surfaces expressing a three-dimensional configuration of “yne” functionalities have been modified with high efficiency and short reaction times using a library of commercially available thiols. Sequential thiol-yne reactions in conjunction with simple UV photolithography has also been described to create micropatterned surfaces.[23] However, the biggest advantages of this reaction are its high efficiency and low toxicity,[24] making it a good candidate for functionalizing biomaterials.

The aim of this study is to evaluate the use of HPGs in the fabrication of PEG-based hydrogels wherein one has the possibility of independently tuning hydrogel biophysical properties or controllably adding bio-functionalities as required. We aim to demonstrate that HPGs can be functionalized with diverse reactive groups to facilitate not only the initial crosslinking reaction but also to enable subsequent modification of the hydrogel network during culture. Here, the hydroxyl groups of HPGs are functionalized with both methacrylate groups that lead to covalent photocrosslinking into the PEG hydrogel network, but also a defined number of alkyne functionalities that are readily available for derivatization with cysteine containing peptides at later reaction times.

EXPERIMENTAL SECTION

Synthesis of functionalized hyperbranched polyglycerols

We use a previously described procedure for the synthesis of the alkyne functionalized HPGs.[15] All reagents were provided by Sigma-Aldrich, St Louis, MO unless otherwise stated.

Hyperbranched polyglycerol (HPG)—Potassium methoxide (25 % by wt. in MeOH) was heated to 60 °C and stirred while adding glycidol (27 eq.) via syringe pump. After 2 h the temperature was increased to 80 °C while glycidol was continuously added. After 24 h, the reaction was cooled to 50 °C, ~60 mL methanol added and stirred until the solution was homogenous. The polymer was precipitated with diethylether, centrifuged and the top layer removed, then re-dissolved in methanol and re-precipitated. Molecular weight was determined by NMR and SEC.

Hyperbranched polyglycerol alkyne (HPG-alkyne)—HPG as a solution (110 mg/mL) in dry DMF was added to NaH (60 % dispersion in mineral oil, 12 eq.) and stirred. Propargyl bromide (80% sol. in toluene, 15 eq.) was added and the reaction allowed to stir overnight under nitrogen. The polymer was precipitated with diethylether and centrifuged. The supernatant was removed and the polymer was re-dissolved in methanol and re-precipitated with diethylether. The number of alkyne groups was determined by ^{1}H NMR.

Hyperbranched polyglycerol methacrylate (HPGMA)[16]—HPG or HPG-alkyne was dried under high vacuum overnight, then dissolved in dry DMSO. DMAP (4 eq.) and glycidyl methacrylate (8.9 eq.) were added to the reaction and allowed to stir overnight at room temperature. The polymer was precipitated with diethylether and centrifuged. The supernatant was removed and the polymer re-dissolved with methanol and re-precipitated with diethylether. The degree of substitution was determined by ^{1}H NMR.

Hydrogel preparation

HPGMA or HPGMA / PEGDA (MW 5K, Jenkem Technology USA, Plano, TX) (50/50) was dissolved in phosphate buffer solution (PBS, pH 7.4) containing 0.05 wt% LAP photoinitiator (PI, lithium phenyl-2,4,6-trimethylbenzoylphosphinate).[25] The prepolymer solution was injected into a 5 mm diameter × 1 mm deep Teflon mold and polymerized under UV light (365nm, 10 mW/cm^2) for 2 min. A 0.5 mg/ml solution of FITC-Arg - Gly - Asp - Ser -Cys - NH2 (FITC-RGDSC) or TAMRA-RGDSC (Bachem - American peptide company, Bubendorf, Switzerland) in the presence of LAP was added to the hydrogel and incubated at room temperature for 1 hour in the dark. Samples were irradiated with UV light for 2 min. Control samples were irradiated in the presence of PI solution without RGDSC. Finally, samples were washed in fresh phenol free media (Invitrogen, Carlsbad, CA).

Mechanical properties, swelling ratio and diffusion

Mechanical and diffusion analyses were performed on fully swollen disks. Specimens were tested in compression at room temperature via an MTS Insight mechanical testing apparatus (Eden Prairie, MN) at a rate of 20% strain/min. The compressive modulus was determined

from the linear region corresponding to ~0–5% strain as previously described.[26] Swelling ratio was calculated by gravimetric measurements.[27] The hydrogel sample was swollen to equilibrium at room temperature, removed, quickly blotted free of surface water using filter paper, then weighed on an analytical balance. The swelling ratio was calculated as the swollen weight of the sample relative to its dry weight. The diffusion coefficient was measured using a fluorescence recovery after photobleaching (FRAP) assay, used extensively to the assess diffusion of proteins within photopolymerized hydrogel networks.[28] Hydrogel disks were fabricated as described above, and then soaked in a 5 mg ml^{-1} FITC-dextran (40 kDa and 4kDa, Sigma-Aldrich) solution for 24 hours at room temperature. After gelation, the FRAP assay was performed using a multi-photon confocal microscope equipped with a FRAP module (LSM 710 NLO, Zeiss) in order to calculate construct diffusion coefficient ($\mu m^2\ s^{-1}$). Here, the 488 nm laser was used to photobleach a circular spot (radius 85 μm, NA 0.16, 80 s) within the construct; time lapse imaging (every 2 s for 3 min) of the fluorescent intensity within that region was monitored to quantify the return of fluorescence due to the diffusion of FITC-dextran from the surrounding gel regions. The normalized fluorescence recovery curve is calculated setting fluorescence intensity before beaching to 1. A reduction of the bleaching time (3 to 5 s), was used to prove that the effect of diffusion during the photobleaching process is negligible (Table S1).[29] The relationship between diffusion coefficient (D) and diffusion time (τ) is based on a 2D diffusion equation described by Axelrod et al.: $\tau_{1/2} = \omega^2\gamma / 4D$ (1), where ω is the radius of the focused circular laser beam (R=85 μm) and γ is a correction factor for the amount of bleaching. FRAP data (Fluorescence vs time, Figure S1) was fitted to $F = A - A \exp(-\tau \cdot t)$, where A is the mobile fraction (calculated by comparing the fluorescence (F) after full recovery with that before bleaching and just after bleaching). Diffusion time ($\tau_{1/2}$) indicates the time at which half of the fluorescence has recovered (A/2), therefore when F = A/2, $\tau_{1/2}=\ln 0.5/-\tau$ (2). Then from equation (1) and (2) diffusion coefficient can be calculated.[30] Braeckmans et al.[28] demonstrate that for objective lenses of low numerical aperture (NA < 0.2) the 3D equation for a disk bleached by a scanning beam reduces to simpler 2D formula for uniform disk bleached by a stationary beam. The thicknesses of the hydrogels used are: P1 2.35 mm, HP2 1.95 mm and H2 2.04 mm.

Patterning

An experimental cell was assembled consisting of two glass substrates, coupled and spaced at 100 μm. The bottom pre-cleaned glass substrate was coated with 3-(trimethoxysilyl) propyl methacrylate (Sigma-Aldrich, St. Louis, MO) by vapor deposition. The hydrogel solution consisted of PEGDA and/or HPGMA supplemented with 0.05 wt% LAP photoinitiator and dissolved in PBS. The cell was filled by capillarity with the hydrogel mixture and irradiated for 90 s with UV light (AccuCure Spot ULM-3-365, Digital Light Lab, 8 mW/cm^2). After separating the substrates, hydrogels remained attached to the adhesive side and TAMRA- / FITC-RGDSC solution (0.5 mg/ml) was added. Then UV light was irradiated again through a photomask for 60 s and substrates were subsequently washed with PBS for 45 min. Then fluorescent patterns were imaged using confocal microscope (LSM 710 NLO, Zeiss). Patterning in thicker hydrogels was performed in a similar manner, and fidelity at the top and bottom surfaces of a hydrogel photopatterned with 165 μm stripes

was confirmed qualitatively by visualization with confocal microscope LSM 710 (Figure S2).

Cell culture

Porcine adipose-derived stem cells (ASCs), a gift of Dr. Matthew Wheeler (U. Illinois)[31] were cultured in DMEM medium supplemented with 10% FBS and penicillin/streptomycin (100 U/ml and 100 μg/ml) at 37 °C in a 5% CO_2 environment. For hydrogel cultures, ASCs were homogeneously mixed with the liquid hydrogel precursor solution in PBS (4 million cells/ml), and the solution photopolymerized as described above. Cell-seeded hydrogels were incubated in cell culture medium at 37 °C, 5% CO_2 on an orbital shaker plate in low adhesion well plates.

Analysis of cell viability and proliferation

Cell viability was observed using a laser scanning confocal microscope (Zeiss LSM710). Prior to imaging, gels were incubated in PBS containing 4 mM calcein AM (λ_{em} = 515 nm, Invitrogen) to stain viable cells. Cell proliferation was additionally quantified using the dimethylthiazoldiphenyltetrazolium bromide (MTT) assay (Vybrant®, Thermo Fisher Scientific) following manufacture's protocol.[32] Blank hydrogels without cells were used as control.

Statistical analysis

All analyses were performed using a one-way analysis of variance (ANOVA) followed by Tukey's HSD post-hoc test. Significance level was set at $p < 0.05$. At least n = 3 samples were examined for hydrogel mechanical and diffusion coefficient assays and n = 3 samples for cell viability and metabolic activity assays. Error was reported in figures as the standard deviation unless otherwise noted.

RESULTS AND DISCUSSION

Independent tailoring of hydrogel modulus and diffusion

The ability to independently alter hydrogel modulus and network structure is important in understanding how biomaterials impact cell behavior. Highly branched polymers possess the potential to facilitate multiple independent crosslinking steps via disparate functionalization of their multiple end groups, keeping a relatively low molecular weight compact structure. In this study, unconfined compression tests were used to examine the effects of composition and HPG MW on hydrogel elastic modulus. Similar to recent work by Cosgriff-Hernandez et al. that incorporated a multifunctional PEG crosslinker into a PEG hydrogel in order to decouple mesh size and elastic modulus,[9] we sought to use HPG-MA to facilitate local changes in crosslinking density, measured via elastic modulus, without disturbing network mesh size, measured via FRAP. The lack of polymeric chain entanglement in HPG polymers, due to its globular shape and resultant increased solubility and reduced viscosity compared to linear analogs,[33] suggests the potential to form variants with lower swelling ratios. Comparatively, PEGDA hydrogels are highly permeable, and their physical properties can be tuned easily to obtain a range of elasticities and pore sizes.[34] The combination of appropriate architecture, functionality and concentration of HPGs in PEGDA was expected

to provide materials that allow for independent alteration of elastic modulus and diffusion (Figure 1).

We hypothesized the addition of HPGMA crosslinkers to PEGDA hydrogels would provide an avenue to decouple compressive modulus and mesh size (swelling ratio). Due to the complications associated with quantifying hydrogel mesh size via SEM, we employed measures of swelling ratio and diffusive transport (FRAP) as quantitative indication of hydrogel mesh size. We first observed that whereas HPGMA polymers alone were able form stable crosslinked networks at high concentrations (20 wt%), they were unable to do so at reduced concentrations (*e.g.*, 10 wt%). This response is likely an effect of the globular structure of the HPG that reduces the polymerization rate and may not reach sufficient crosslinking density to compensate the high swelling of the hydrophilic network, consistent with photopolymerization kinetics of multifunctional monomers.[35] Further, overall trends suggested the hydrogel network properties were dependent on the polymer concentration, with higher concentrations (20 wt%) resulting in stiffer and less swelled gels (Figure 2b).

We subsequently investigated the effect of HPG molecular weight and degree of functionalization on the resultant hydrogel physical properties. We have focused on 2 HPG variants (2,300 vs. 4,200 Da; Table 1) with the same number of methacrylate groups per macromonomer. Interestingly, whereas a significant decrease in swelling ratio was observed in PEG-HPG hydrogels (2,300 Da HPG, 10 wt%) as compared to PEG only variants, no significant difference in elastic modulus was observed (Figure 2a). Operating at higher concentrations (20 wt%), incorporation of 2,300 Da HPGMA into the PEGDA polymer network results in a synergistic increase in mechanical properties. Here, the elastic modulus of PEGDA-HPGMA hydrogels increases more than 2-fold compared to PEGDA alone and 8-fold compared to HPGMA alone (Figure 2b). However, changes in swelling ratio are much smaller (8.2 vs. 7.1 vs. 6.7 for PEGDA, HPGMA + PEGDA and HPGMA hydrogels, respectively), with no significant difference in swelling ratio between HPGMA hydrogels alone and the HPGMA - PEGDA composite.

Hydrogels incorporating larger molecular weight HPGMA (4,200 Da; H2, HP2 hydrogels) did not show synergistic increase in modulus when copolymerized with PEGDA, but rather showed reduced modulus, likely a result of the decreased concentration of MA reactive groups, (Figure 2c). Interestingly, when comparing HP2 (HPGMA - PEGDA) vs. PEGDA mechanical properties and corresponding diffusion coefficient we observe that, although modulus significantly decreases from 174 to 36 kPa with the inclusion of HPGMA in the network, the diffusion coefficient stays constant around 40 $\mu m^2/s$. Diffusion rates of dextran molecules through HPGMA hydrogels alone (H2) and swelling ratio are significantly lower than corresponding PEG hydrogels, likely as a result of increased presence of hydrophobic methacrylate moieties.[16] These results may also be ascribed to a combination of reduced crosslinking density and the less compact structure of the HPG which enlarges the microporous structure.[27]

Together, these results demonstrate that hydrogel elastic modulus can be significantly manipulated independent of swelling ratio and diffusivity, via selective alterations of hydrogel crosslinking density introduced by low molecular weight HPGMA into PEGDA

hydrogel networks. With the addition of HPGs to PEGDA hydrogels we can obtain the necessary mechanical properties while keeping pore sizes that enable prolonged viability of encapsulated cells without negative effects of decreases in diffusion.[36] The effect of HPGMA was more pronounced in more concentrated samples (Figures 2b, 2c vs. 2a), likely a result of increased crosslinking densities.

Hydrogel patterning with bioactive molecules

Click chemistry has enabled several critical advances in biomaterials design, for example, allowing hydrogel parameters to be tuned efficiently in real time using straightforward procedures.[2] Here, we used a two-step protocol to sequentially fabricate biomolecule-functionalized, crosslinked hydrogels. In the primary step, a uniform hydrogel was formed using UV photopolymerization between multi-methacrylate HPG macromonomers and bifunctional PEGDA in the presence of a photoinitiator (Figure 3a). Monofunctional, pendant RGDSC-containing peptides were subsequently added in a second step to demonstrate the selective addition of cell adhesion moieties within the hydrogel after hydrogel network crosslinking (Figure 3b). In this secondary step, hydrogels were exposed to UV light to react cysteine thiol groups to HPG alkyne groups and remaining methacrylate groups from the first step. Patterns are obtained by using a photomask. The radical-mediated reaction of a thiol with an alkyne generates a dithioether adduct (Figure 3c). These alkyne-thiol patterning techniques have been used previously in 2D surfaces for cells culture,[37] via a two-step reaction involving the addition of the thiyl radical to the C≡C bond, yielding an intermediate vinyl sulfide species that subsequently forms the 1,2-dithioether adduct by undergoing a second, formal thiol-ene reaction.[21] These thiol-yne reactions were carried out in the presence of LAP at 365 nm, with subsequent analysis of the resultant biomolecule patterns with the hydrogel via fluorescence (Figure 4a). Notably, increased RGDSC-FITC immobilization was observed in HPGMA decorated with alkynes (0.2M) vs. PEGDA or HPGMA with no alkynes. High conversion of methacrylate groups in the initial crosslinking reaction, plus methacrylate groups being amongst the least reactive alkenes[38], is likely responsible for poor uptake of RGD groups. However, the addition of alkyne groups orthogonal to the initial photopolymerization reaction, provides a strategy for improved biomolecule incorporation.

We subsequently examined combinations of methacrylate and alkyne groups in HPGMA hydrogels to increase RGD peptide patterning efficiency. For this purpose, we synthesized a library of multiple HPGs with different molecular weights and different degrees of methacrylate and alkyne functionalization (Table 2). We observe that a medium concentration of 0.2M alkyne groups is necessary to obtain the most effective covalent bonding of RGD (Figure 4b). Network methacrylate concentration also plays an important role, as low concentrations (0.1M) result in hydrogels with poor mechanical properties (Table 2), especially when the alkyne concentration is high. This occurrence is likely related to a phase separation during the polymerization caused by an increase in hydrophobic domains.[39] Further, when both methacrylate and alkyne concentrations were high (sample 9, Table 2), the increased density of the hydrogel network architecture reduced patterning efficiency. Together, these data demonstrate that HPGMA macro monomers functionalized with alkynes provide the opportunity to create spatial patterns of biomolecules within the

hydrogel network via sequential crosslinking and biomolecule patterning reactions. Additionally, H1 and HP1 hydrogels (Table 1) have also been patterned with FITC-RGDSC peptides (Figure S3). Ongoing efforts are exploring the use of sequential and space-selective thiol-yne modifications using photopatterning to create more complex biomolecular patterns consistent with the heterogeneity of biological tissues. These approaches include the use of orthogonal gradients and the patterning and multi-component patterning of biomolecules at desired time points.

Viability and metabolic activity of encapsulated cells

We subsequently examined whether enhanced patterning of RGD within the HPGMA-alkyne hydrogels translated to changes in cellular behavior. Based on the well-defined multi-lineage specification capacity of porcine adipose derived stem cells (pASCs) in response to biomolecular cues,[31, 40, 41] our laboratory has employed pASCs for a wide range of tissue engineering applications using both scaffold and hydrogel-based biomaterials.[42–45] As a result, we examined the viability of pASCs within the new class of hydrogels reported here. We encapsulated porcine ASCs within the hydrogel networks with or without the addition of ubiquitous RGD sequence (Figure 3a). Live/dead staining after 48 h in culture suggests that ASCs remain alive after encapsulation and that, as expected, hydrogels incorporating RGD show increased cell content (Figure 5). Examining TAMRA florescence demonstrates that TAMRA-RGDSC remains covalently bonded to the hydrogel network for HPGMA and HPGMA-PEGDA hydrogels. In comparison, the TAMRA peptides are localized on the cell surface or were internalized by ASCs in the PEGDA hydrogels, likely resulting from the lack of available reactive sites to immobilize TAMRA-RGDSC within the PEGDA hydrogel. Examining the metabolic activity of the overall cell cultures via MTT, we observed ASCs show enhanced cell activity in RGD-functionalized HPGMA alone and HPGMA - PEGDA hydrogel (Figure 6). However, ASCs did not show heightened metabolic activity after the inclusion of RGD, likely as the PEGDA hydrogels did not facilitate RGD immobilization within the hydrogel network. Together, these findings suggest that light based reactions can be employed with HPGMA-functionalized hydrogels to covalently incorporate adhesive ligands, and likely a wider range of biomolecules such as growth factors, within the hydrogel network at discrete time points and locations within the cell-laden hydrogels.

CONCLUSIONS

This work highlights how the unique properties of hyperbranched polyglycerols facilitate a decoupled manipulation of hydrogel stiffness and diffusion while also enabling spatiotemporal control of biomolecules patterning within the polymerized hydrogel network. The diversity of responses achieved via mixtures of HPGMA and PEGDA suggest future opportunities to tailor HPGMA molecular weight and concentration to expand and refine the range of achievable biophysical properties. Importantly, we demonstrate the use of simple chemistries that can be performed in the presence of living cells. The resulting platform provides a systematic way of manipulating biophysical and biomolecular properties of extracellular matrix analogs to better understand the interactions between cells and their microenvironment.

Supplementary Material

Refer to Web version on PubMed Central for supplementary material.

Acknowledgments

The authors acknowledge Carl R. Woese Institute for Genomic Biology Core Facilities for assistance with fluorescence imaging, Dr. Matthew Wheeler (University of Illinois) for the gift of porcine adipose derived stem cells, and Prof. Hyunjoon Kong (University of Illinois) for access to equipment to analyze mechanical properties of hydrogels. This material is based upon work supported by the National Science Foundation under Grant No. CBET-1254738 (B.A.C.H.) and CHE-1307404 (S.C.Z.). Research reported in this publication was supported by the National Institute of Diabetes and Digestive and Kidney Diseases of the National Institutes of Health under Award Number R01 DK099528 (B.A.C.H). The authors are grateful for additional funding provided by the Illini 4000, as well as the Department of Chemical & Biomolecular Engineering and the Carl R. Woese Institute for Genomic Biology at the University of Illinois at Urbana- Champaign.

References

1. Yang C, Tibbitt MW, Basta L, Anseth KS. Mechanical memory and dosing influence stem cell fate. Nat Mater. 2014; 13(6):645–52. [PubMed: 24633344]
2. DeForest CA, Anseth KS. Cytocompatible click-based hydrogels with dynamically tunable properties through orthogonal photoconjugation and photocleavage reactions. Nat Chem. 2011; 3(12):925–931. [PubMed: 22109271]
3. Kloxin AM, Tibbitt MW, Kasko AM, Fairbairn JA, Anseth KS. Tunable hydrogels for external manipulation of cellular microenvironments through controlled photodegradation. Adv Mater. 2010; 22(1):61–66. [PubMed: 20217698]
4. Caliari SR, Perepelyuk M, Cosgrove BD, Tsai SJ, Lee GY, Mauck RL, Wells RG, Burdick JA. Stiffening hydrogels for investigating the dynamics of hepatic stellate cell mechanotransduction during myofibroblast activation. Sci Rep. 2016; 6:21387. [PubMed: 26906177]
5. Peyton SR, Raub CB, Keschrumrus VP, Putnam AJ. The use of poly(ethylene glycol) hydrogels to investigate the impact of ECM chemistry and mechanics on smooth muscle cells. Biomaterials. 2006; 27(28):4881–4893. [PubMed: 16762407]
6. Liao H, Munoz-Pinto D, Qu X, Hou Y, Grunlan MA, Hahn MS. Influence of hydrogel mechanical properties and mesh size on vocal fold fibroblast extracellular matrix production and phenotype. Acta Biomater. 2008; 4(5):1161–1171. [PubMed: 18515199]
7. Bryant SJ, Chowdhury TT, Lee DA, Bader DL, Anseth KS. Crosslinking density influences chondrocyte metabolism in dynamically loaded photocrosslinked poly (ethylene glycol) hydrogels. Ann Biomed Eng. 2004; 32(3):407–417. [PubMed: 15095815]
8. Anseth KS, Bowman CN, Brannon-Peppas L. Mechanical properties of hydrogels and their experimental determination. Biomaterials. 1996; 17(17):1647–1657. [PubMed: 8866026]
9. Browning MB, Wilems T, Hahn M, Cosgriff-Hernandez E. Compositional control of poly(ethylene glycol) hydrogel modulus independent of mesh size. J Biomed Mater Res, Part A. 2011; 98A(2): 268–273.
10. Frey H, Haag R. Dendritic polyglycerol: a new versatile biocompatible material. Rev Mol Biotechnol. 2002; 90(3–4):257–267.
11. Calderón M, Quadir MA, Sharma SK, Haag R. Dendritic Polyglycerols for Biomedical Applications. Adv Mater. 2010; 22(2):190–218. [PubMed: 20217684]
12. Zhu J. Bioactive modification of poly(ethylene glycol) hydrogels for tissue engineering. Biomaterials. 2010; 31(17):4639–4656. [PubMed: 20303169]
13. Zhang H, Patel A, Gaharwar AK, Mihaila SM, Iviglia G, Mukundan S, Bae H, Yang H, Khademhosseini A. Hyperbranched Polyester Hydrogels with Controlled Drug Release and Cell Adhesion Properties. Biomacromolecules. 2013; 14(5):1299–1310. [PubMed: 23394067]
14. Pedrón S, Peinado C, Bosch P, Anseth KS. Synthesis and characterization of degradable bioconjugated hydrogels with hyperbranched multifunctional cross-linkers. Acta Biomater. 2010; 6(11):4189–4198. [PubMed: 20561601]

15. Zill A, Rutz AL, Kohman RE, Alkilany AM, Murphy CJ, Kong H, Zimmerman SC. Clickable polyglycerol hyperbranched polymers and their application to gold nanoparticles and acid-labile nanocarriers. Chem Commun. 2011; 47(4):1279–1281.
16. Oudshoorn MHM, Rissmann R, Bouwstra JA, Hennink WE. Synthesis and characterization of hyperbranched polyglycerol hydrogels. Biomaterials. 2006; 27(32):5471–5479. [PubMed: 16859743]
17. Oudshoorn MHM, Penterman R, Rissmann R, Bouwstra JA, Broer DJ, Hennink WE. Preparation and Characterization of Structured Hydrogel Microparticles Based on Cross-Linked Hyperbranched Polyglycerol. Langmuir. 2007; 23(23):11819–11825. [PubMed: 17927225]
18. Steinhilber D, Seiffert S, Heyman JA, Paulus F, Weitz DA, Haag R. Hyperbranched polyglycerols on the nanometer and micrometer scale. Biomaterials. 2011; 32(5):1311–1316. [PubMed: 21047679]
19. Khetan S, Burdick JA. Patterning network structure to spatially control cellular remodeling and stem cell fate within 3-dimensional hydrogels. Biomaterials. 2010; 31(32):8228–8234. [PubMed: 20674004]
20. DeForest CA, Polizzotti BD, Anseth KS. Sequential click reactions for synthesizing and patterning three-dimensional cell microenvironments. Nat Mater. 2009; 8(8):659–664. [PubMed: 19543279]
21. Fairbanks BD, Scott TF, Kloxin CJ, Anseth KS, Bowman CN. Thiol−Yne Photopolymerizations: Novel Mechanism, Kinetics, and Step-Growth Formation of Highly Cross-Linked Networks. Macromolecules. 2009; 42(1):211–217. [PubMed: 19461871]
22. Lowe AB. Thiol-yne 'click'/coupling chemistry and recent applications in polymer and materials synthesis and modification. Polymer. 2014; 55(22):5517–5549.
23. Hensarling RM, Doughty VA, Chan JW, Patton DL. "Clicking" Polymer Brushes with Thiol-yne Chemistry: Indoors and Out. J Am Chem Soc. 2009; 131(41):14673–14675. [PubMed: 19778016]
24. Hoyle CE, Lowe AB, Bowman CN. Thiol-click chemistry: A multifaceted toolbox for small molecule and polymer synthesis. Chem Soc Rev. 2010; 39(4):1355–1387. [PubMed: 20309491]
25. Fairbanks BD, Schwartz MP, Bowman CN, Anseth KS. Photoinitiated polymerization of PEG-diacrylate with lithium phenyl-2,4,6-trimethylbenzoylphosphinate: polymerization rate and cytocompatibility. Biomaterials. 2009; 30(35):6702–6707. [PubMed: 19783300]
26. Pedron S, Harley BAC. The impact of the biophysical features of a 3D gelatin microenvironment on glioblastoma malignancy. J Biomed Mater Res, Part A. 2013; 101(12):3405–15.
27. Keys KB, Andreopoulos FM, Peppas NA. Poly(ethylene glycol) Star Polymer Hydrogels. Macromolecules. 1998; 31(23):8149–8156.
28. Braeckmans K, Peeters L, Sanders NN, De Smedt SC, Demeester J. Three-Dimensional Fluorescence Recovery after Photobleaching with the Confocal Scanning Laser Microscope. Biophys J. 2003; 85(4):2240–2252. [PubMed: 14507689]
29. Meyvis TKL, De Smedt SC, Van Oostveldt P, Demeester J. Fluorescence Recovery After Photobleaching: A Versatile Tool for Mobility and Interaction Measurements in Pharmaceutical Research. Pharmaceutical Research. 1999; 16(8):1153–1162. [PubMed: 10468014]
30. Reits EA, Neefjes JJ. From fixed to FRAP: measuring protein mobility and activity in living cells. Nat Cell Biol. 2001; 3(6):E145–7. [PubMed: 11389456]
31. Monaco E, Bionaz M, Rodriguez-Zas S, Hurley WL, Wheeler MB. Transcriptomics comparison between porcine adipose and bone marrow mesenchymal stem cells during in vitro osteogenic and adipogenic differentiation. PLoS ONE. 2012; 7(3):e32481. [PubMed: 22412878]
32. Pedron S, Becka E, Harley BA. Regulation of glioma cell phenotype in 3D matrices by hyaluronic acid. Biomaterials. 2013; 34(30):7408–17. [PubMed: 23827186]
33. Voit BI, Lederer A. Hyperbranched and Highly Branched Polymer Architectures— Synthetic Strategies and Major Characterization Aspects. Chem Rev. 2009; 109(11):5924–5973. [PubMed: 19785454]
34. Nguyen KT, West JL. Photopolymerizable hydrogels for tissue engineering applications. Biomaterials. 2002; 23(22):4307–4314. [PubMed: 12219820]
35. Andrzejewska E. Photopolymerization kinetics of multifunctional monomers. Prog Polym Sci. 2001; 26(4):605–665.

36. Nuttelman CR, Benoit DSW, Tripodi MC, Anseth KS. The effect of ethylene glycol methacrylate phosphate in PEG hydrogels on mineralization and viability of encapsulated hMSCs. Biomaterials. 2006; 27(8):1377–1386. [PubMed: 16139351]

37. Costa P, Gautrot JE, Connelly JT. Directing cell migration using micropatterned and dynamically adhesive polymer brushes. Acta Biomater. 2014; 10(6):2415–2422. [PubMed: 24508539]

38. Lowe AB. Thiol-ene "click" reactions and recent applications in polymer and materials synthesis. Polym Chem. 2010; 1(1):17–36.

39. Wang DK, Hill DJT, Rasoul FA, Whittaker AK. Synthesis of a new hyperbranched, vinyl macromonomer through the use of click chemistry: Synthesis and characterization of copolymer hydrogels with PEG diacrylate. J Polym Sci, Part A: Polym Chem. 2012; 50(6):1143–1157.

40. Bionaz M, Monaco E, Wheeler MB. Transcription adaptation during in vitro adipogenesis and osteogenesis of porcine mesenchymal stem cells: dynamics of pathways, biological processes, up-stream regulators, and gene networks. PLoS ONE. 2015; 10(9):e0137644. [PubMed: 26398344]

41. Monaco E, Bionaz M, de Lima AS, Hurley WL, Loor JJ, Wheeler MB. Selection and reliability of internal reference genes for quantitative PCR verification of transcriptomics during the differentiation process of porcine adult mesenchymal stem cells. Stem Cell Res Ther. 2010; 1(1):7. [PubMed: 20504288]

42. Banks JM, Harley BAC, Bailey RC. Tunable, photoreactive hydrogel system to probe synergies between mechanical and biomolecular cues on adipose-derived mesenchymal stem cell differentiation. ACS Biomater Sci Eng. 2015; 1(8):718–25.

43. Banks JM, Mozdzen LC, Harley BAC, Bailey RC. The combined effects of matrix stiffness and growth factor immobilization on the bioactivity and differentiation capabilities of adipose-derived stem cells. Biomaterials. 2014; 35(32):8951–9. [PubMed: 25085859]

44. Mozdzen LC, Rodgers R, Banks JM, Bailey RC, Harley BAC. Increasing the strength and bioactivity of collagen scaffolds using customizable arrays of 3D-printed polymer fibers. Acta Biomater. 2016; 15(33):25–33.

45. Weisgerber DW, Erning K, Flanagan C, Hollister SJ, Harley BAC. Evaluation of multi-scale mineralized collagen-polycaprolactone composites for bone tissue engineering. J Mech Behav Biomed Mater. 2016; 61:318–327. [PubMed: 27104930]

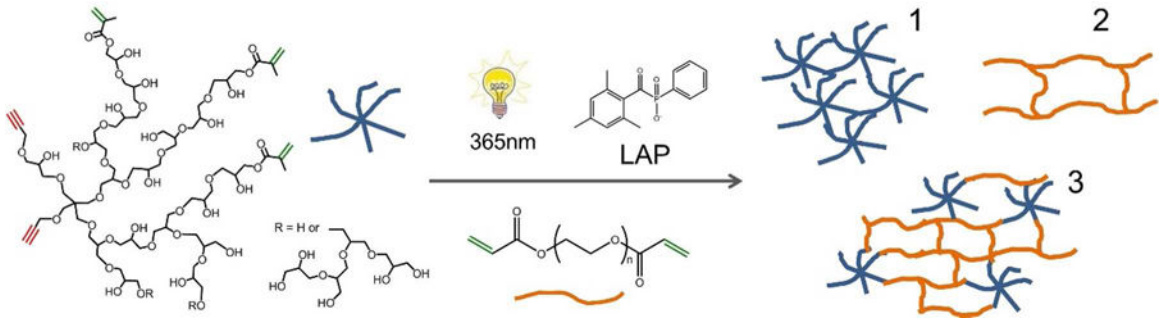

Figure 1.

Schematic representation of HPG functionalization and hydrogel fabrication. HPGs are functionalized with multiple methacrylate and alkyne groups. Copolymerization with PEGDA leads to a unique network structure that features local increases in crosslinking density due to the particular properties of HPGs. (1) HPGMA, (2) PEGDA, (3) HPGMA + PEGDA hydrogels.

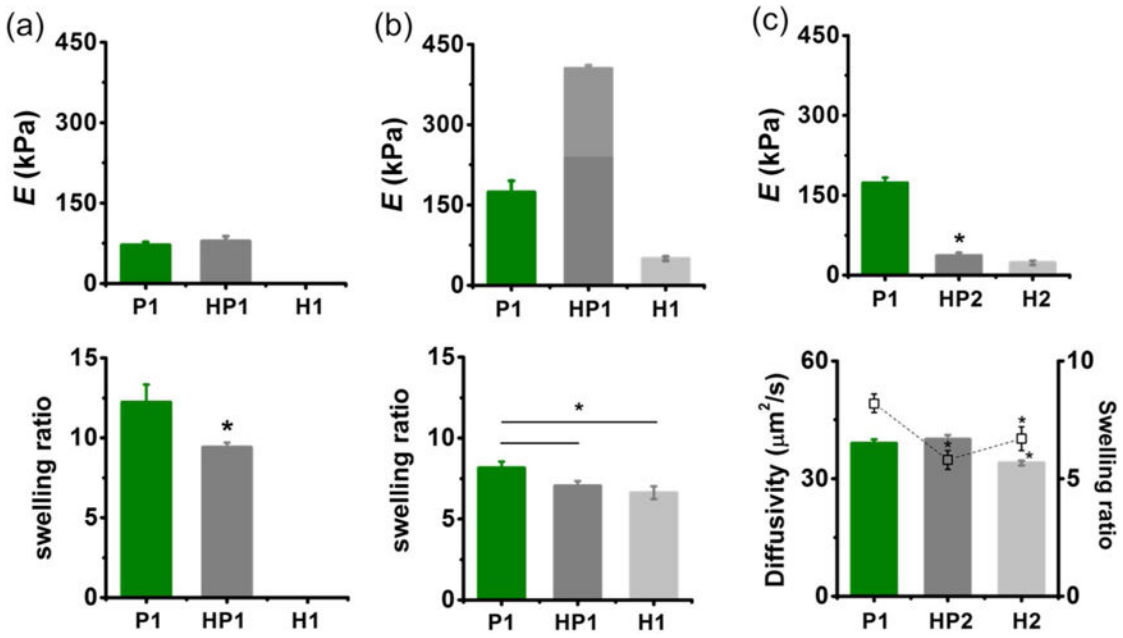

Figure 2.

Hydrogel biophysical properties. Elastic modulus and swelling ratio of HPGMA (H1: MW 2,300, 5 MA), PEGDA (P1: MW 5,000, 2 A), and HPGMA + PEGDA (HP1) copolymer hydrogels. Hydrogels are fabricated with (a) 10 wt% and (b) 20 wt% polymer content. (c) Elastic modulus, diffusion coefficient and swelling ratio of HPGMA (H2: MW 4,200, 5 MA) PEGDA (P1: MW 5,000, 2 A) and HPGMA + PEGDA (HP2; 20 wt%) copolymer hydrogels. Reactive groups concentration decreases from 0.4 to 0.2 M as HPGMA MW increases, directly related to decrease in mechanical properties. Diffusion coefficient ($\mu m^2/s$) of FITC-dextran (40 kDa) molecules within hydrogels (20 wt%) as measured by FRAP. *p< 0.05

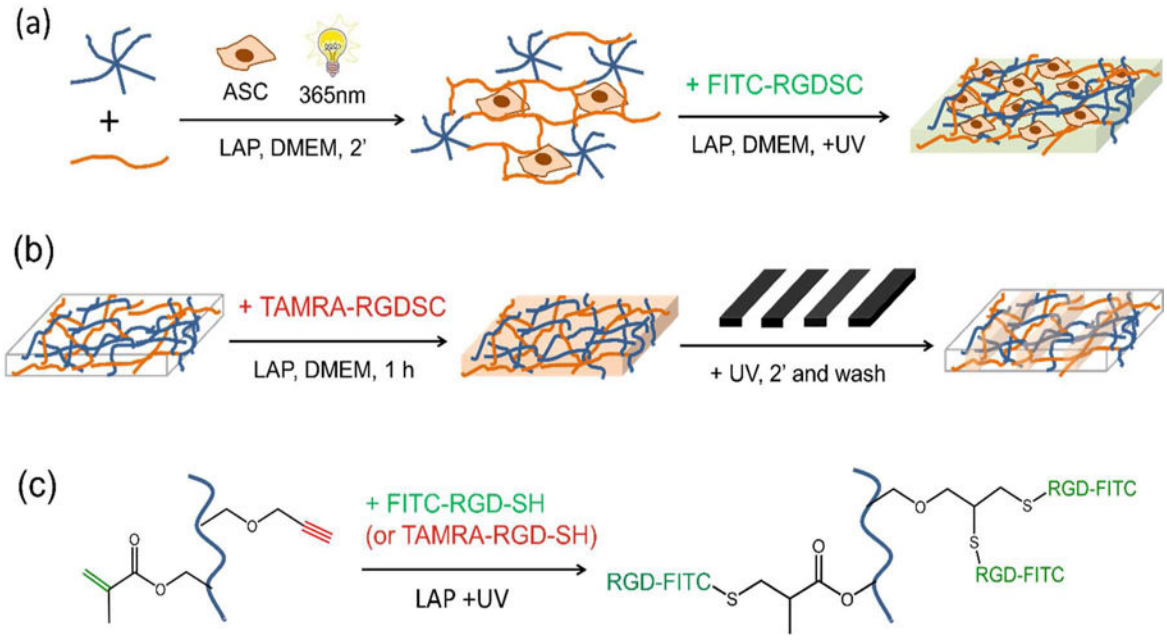

Figure 3.

Patterning of HPG-PEG hydrogels. Schematic representation of (a) ASC encapsulation within HPGMA / PEGDA composite hydrogels prior to functionalization with FITC-RGDSC and (b) TAMRA-RGDSC patterning by UV catalyzed reaction. (c) Representation of thiol-radical initiated "click" reactions for photopatterning "yne"-containing HPGMA polymers with cysteine containing RGDSC peptides. This scheme shows all possible reactions that may occur during the patterning process.

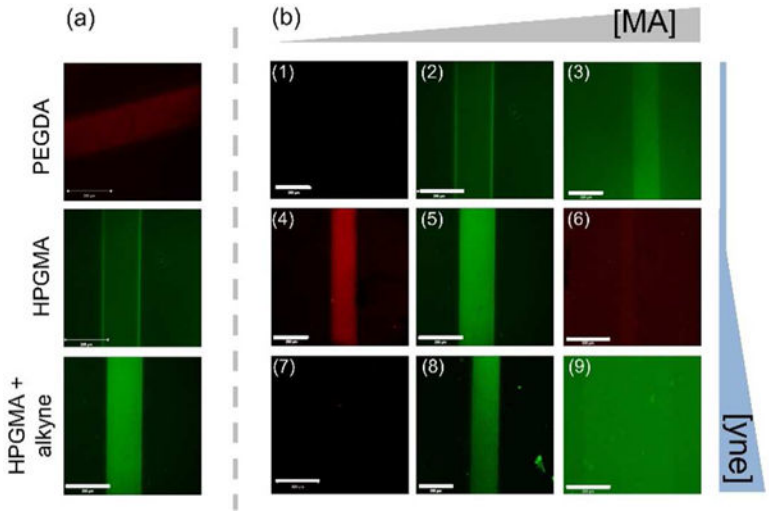

Figure 4.

Hydrogel patterning with FITC or TAMRA-RGDSC peptides. (a) Hydrogel reactivity depends on alkyne and meth/acrylate concentration in HPGMA. (b) The presence of alkyne groups leads to more efficient incorporation of peptides into HPGMA hydrogels. Combinations of MA and alkyne concentrations (1) – (9) are detailed in Table 2. Scale bar 200 μm.

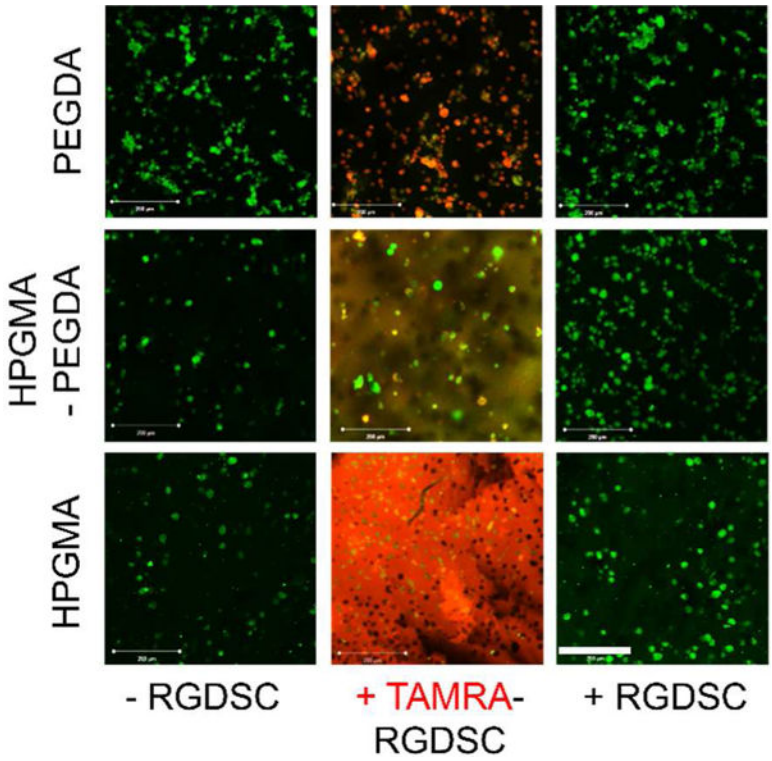

Figure 5.

RGD decorated HPGMA hydrogels affect cell behavior. ASCs cultured within HPGMA, HPGMA - PEGDA and PEGDA hydrogels (20 wt%) as a function of incorporated TAMRA-labeled RGD. The distribution of the TAMRA fluorescent label suggests that RGD was immobilized within hydrogels containing HPGMA. TAMRA clustering at the cell surface in PEDGA hydrogels suggests RGD was not covalently immobilized within the hydrogel network. Cells are stained with Calcein A (green) to account for cell viability. Scale bar 200 μm.

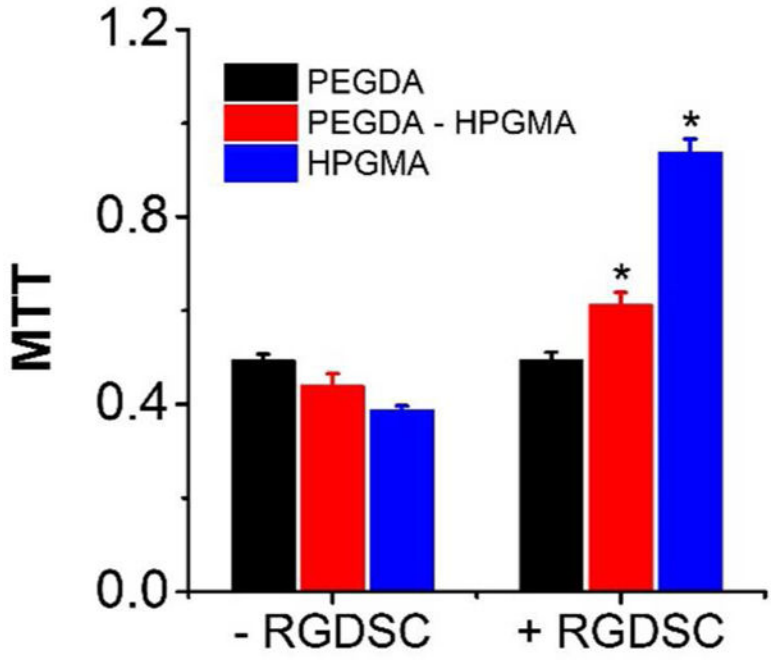

Figure 6.

Metabolic activity of ASCs encapsulated in PEGDA, HPGMA, and HPGMA - PEGDA hydrogels. Significantly increased metabolic activity was observed as a function of incorporated RGDSC. *: $p < 0.05$, between hydrogels of same composition with and without RGDSC.

Table 1

Monomer characteristics and hydrogel composition. Molecular weight of monomers (MW), concentration of total (meth) / acrylate groups (MA/A) in pre-polymer solution with 20 wt% gel concentration, concentration of alkyne groups and Young modulus (*E*).

	Composition	MW_{HPGMA} (Da)	MW_{PEGDA} (Da)	MA/A (M)	Alkyne (M)	E (kPa)
H1	HPGMA	2,300	—	0.43	0.2 / 0.5 *	50 ± 5
HP1	HPGMA-PEGDA	2,300	5,000	0.26	0.1 / 0.3 *	406 ± 3
HP2	HPGMA-PEGDA	4,200	5,000	0.16	0.1	36 ± 5
H2	HPGMA	4,200	—	0.24	0.3	23 ± 2
P1	PEGDA	—	5,000	0.08	—	174 ± 19

* H1 polymers were prepared with two different concentrations of alkyne groups.

Table 2

Characteristics of HPGs used to fabricate patterned hydrogels. Molecular weight of monomers (MW), concentration of total methacrylate groups (MA) in pre-polymer solution with 20 wt% gel concentration and concentration of alkyne groups.

	MW (Da)	MA (M)	Alkyne (M)
1	12,000	0.08	0
2	4,200	0.17	0
3	4,200	0.33	0
4	6,500	0.09	0.17
5	2,300	0.17	0.17
6	12,000	0.30	0.15
7	4,200	0.07	0.24
8	2,300	0.17	0.48
9	4,200	0.29	0.26